CHAPTER 93

Observations of the Swash Expression of Far Infragravity Wave Motions

Rob Holman[1], Peter Howd[1], Joan Oltman-Shay[2], and Paul Komar[1]

Abstract

One of the important results from the recent SUPERDUCK experiment was the discovery of very low frequency motions (10^2 - 10^3 second periods) with anomalously short longshore wavelengths (10^2meters). Subsequent analysis showed the motions to be shear waves, unstable perturbations of the mean longshore current that act to conserve potential vorticity. A specific prediction of the model is that these waves have negligible elevation signal (they are non-divergent), in contrast to gravity waves. Examination of simultaneous run-up data confirms the non-divergent nature of the solutions. While edge wave modes were detected, no significant swash energy was seen in the low frequency, high wavenumber region where shear wave energy was found in the current meter data. This apparently negative result adds support to the interpretation of these motions as shear waves.

Introduction

In September and October, 1986, a large field experiment called SUPERDUCK was held at the U.S. Army Corps of Engineers Field Research Facility (FRF) at Duck, North Carolina, USA. The site features a pronounced and frequently active nearshore sand bar system, and a primary objective of the October phase of the experiment was to study possible mechanisms of sand bar generation. Of particular interest to some participants was validation of models that depend on the presence of edge waves to account for dominant longshore lengthscales.

Detection of edge waves was accomplished using a longshore array of bi-directional electromagnetic current meters placed 50 m offshore, in the expected location of the trough, landward of the bar. Seven instruments were placed with lag spacings of 110, 20, 30, 10, 70, and 50 m, an optimal design for the subsequent maximum likelihood spectral analysis. Four hour time series were collected, and frequency-wavenumber (f-k) spectra computed.

1. College of Oceanography, Ocean Admin Bldg 104, Oregon State University, Corvallis, OR, USA 97331-5503
2. Quest Integrated, 21414 68th Ave. So., Kent WA, USA 98032

While edge wave modes were observed in the infragravity band, the highest energy densities occurred at lower frequencies with periods typically on the order of 10^2 - 10^3 seconds (Oltman-Shay *et al*, 1989). To distinguish this frequency band, the name Far InfraGravity (or FIG) band was adopted, in analogy to the relationship of infrared and far infrared light in the optical spectrum. Most surprising, the wavenumbers of the FIG energy were substantially higher than $\sigma^2/g\beta$, the wavenumber of a mode 0 edge wave, the largest value allowable for gravity waves (σ is radial frequency, g the acceleration of gravity, and β the beach slope). Moreover, the observed motions were very coherent and were always progressive in the direction of the mean longshore current.

A theoretical explanation of these motions was provided by Bowen and Holman (1989). They showed that under some circumstances a strong mean longshore current is unstable to perturbations, such that the perturbation will grow and progress with the current. These motions are called shear waves since their existence depends on the cross-shore shear structure of the current. Using a simple example geometry, Bowen and Holman showed that typical time and length scales of shear waves would be in the FIG band, and at high wavenumber, as was observed in the data.

The underlying dynamics of shear waves depend on the conservation of the total potential vorticity. Thus, a perturbation of the vorticity (shear) of the mean longshore current will be compensated for by the relative vorticity, resulting in a meandering flow pattern. However, an explicit assumption of the theory is that the motions are non-divergent (the rigid lid assumption) so that the rate of change of sea surface elevation is negligible. Thus, the theory specifically predicts that, despite the large energies seen in the velocity data, the sea surface elevation signal of shear waves should be negligible.

Synchronous with the velocity data, run-up measurements were also collected during SUPERDUCK. These data represent sea surface elevation signals at a specific location (the shoreline), so they can be used to test the non-divergent assumption and hence whether the observed motions are, in fact, shear waves. Thus the objective of this paper is to examine swash data to determine the presence or absence of energy at the low frequencies and high wavenumbers seen by the current meter data. A negative result adds support to the interpretation of these waves as non-divergent shear waves.

Field Experiment

Run-up data were collected during SUPERDUCK using videotapes of nearshore wave motion (note that the terms run-up and swash are used interchangeably in this paper to indicate the time series of sea surface elevation at the shoreline). Three cameras were mounted on the top of a high tower on the crest of the sand dune, 43.2 m above mean sea level. Records were 1 hour 55 minutes long and, when possible, were timed to correspond to current meter runs.

Digitization of the swash time series was carried out with an Imaging Technology Series 150 image processing package using the following set of steps. As a

preliminary step, the geometry of the camera view was solved for by digitizing a representative frame and then locating the image coordinates of a set of known ground control points that fall in the field of view. The problem is generally over-determined (more known points than unknown parameters) so that the geometry variables can be solved for in a least squares sense. Then, for each sampling time, the video frame is digitized and the beach profile transects of interest placed on the image, based on the now-known geometry. Figure 1 shows an example frame. A total of 39 transects have been placed on the image at a longshore spacing of 10 m (for a total longshore beach length of 380 m being analyzed). For each transect, the intensities of image pixels are read into the host Sun 4/110 computer and a search algorithm implemented to find the water's edge (the selected run-up location is marked on the screen and in figure 1 with a small vertical tick). This selected horizontal location is then translated into a vertical elevation swash signal based on the measured beach profile, and the resulting value written into the computer file. This search is performed for each of the 39 transects before a new frame is digitized. The whole process is repeated every second for the length of the run. An operator monitors the performance of the system by observing the marked computer "picks" and can tune algorithm parameters for each individual transect during digitization.

Resolution of the technique depends on range from the camera and focal length of the individual lens. Typical horizontal resolutions range from 20 cm (swash elevation of 2.0 cm) for close ranges to 0.73 m (swash elevation of 7.3 cm) for the most distant cases. Worst case resolutions for each of the analyzed runs are listed in Table 1.

Four data runs were selected for analysis. The first two were at times when no significant shear wave energy was observed in the current meter records and the second two when shear wave energy was obvious. Times of the runs and associated environmental conditions are listed in Table I.

Table I

Statistics for Selected Data Runs

Name	time (EST)	date	T^1 (sec)	α^2 (°)	H_s^3 (m)	R_s^4 (m)	R_s/H_s	δx^5 (m)
GD097	1135	10/12/86	11.4	+14	2.18	2.47±.47	1.13	0.68
GD105	0745	10/13/86	10.7	+22	1.52	1.78±0.22	1.17	0.73
GM133	1025	10/15/86	6.2	-28	1.34	1.35±0.14	1.01	0.37
GM143	1020	10/16/86	5.0	-50	1.27	1.18±0.14	0.93	0.37

1. peak period from 8 m depth pressure sensor
2. peak direction from 8 m depth linear pressure sensor array. Positive angles from south
3. significant wave height from 8 m depth pressure sensor, (periods from 3 - 20 sec)
4. significant swash height, averaged over entire longshore run-up array
5. horizontal resolution of swash data at farthest transect (worst case)

Figure 1. Example video frame showing waves in the nearshore and run-up. Lines across the beach represent surveyed beach profiles. For automatic digitization, the computer searches out along each line (starting with the left hand tick) until it finds the run-up (marked by the right-hand tick). 39 transects are shown.

General Swash Results

Figure 2 shows an example section of swash time series for 32 of the 39 transects, a total beach length of 310 m. The longshore structure of individual swashes is apparent to the eye; there is little discernible phase lag through the array, implying that the waves were approaching the shoreline at near normal incidence (nearby transects actually appear to lead distant ones slightly, implying a northward propagation, consistent with the observed angle of incidence). The visible coherence with longshore distance lends confidence to the digitization process; longshore variability appears to be a function of the observed wave field, not random noise in the sampling algorithm.

A further check on the believability of the results comes from plotting the longshore variability of the basic time series statistics. Figure 3 shows the significant swash height (calculated as 4 * standard deviation) for each of the four runs. Longshore-averaged values are listed in Table I as dimensional values as well as normalized by the significant wave height measured by offshore pressure sensors. In general, the longshore variability shown in figure 3 is quite small, implying a stability in the digitization process. Most variability that does exist occurs on a number of transects, as would be expected for a natural phenomenon (as opposed to random scatter of the digitizing process). It should be noted that in none of these runs was the beach completely two dimensional. In each case, there was natural longshore variability in the bathymetry that undoubtedly contributed to the variability in the observed swash statistics.

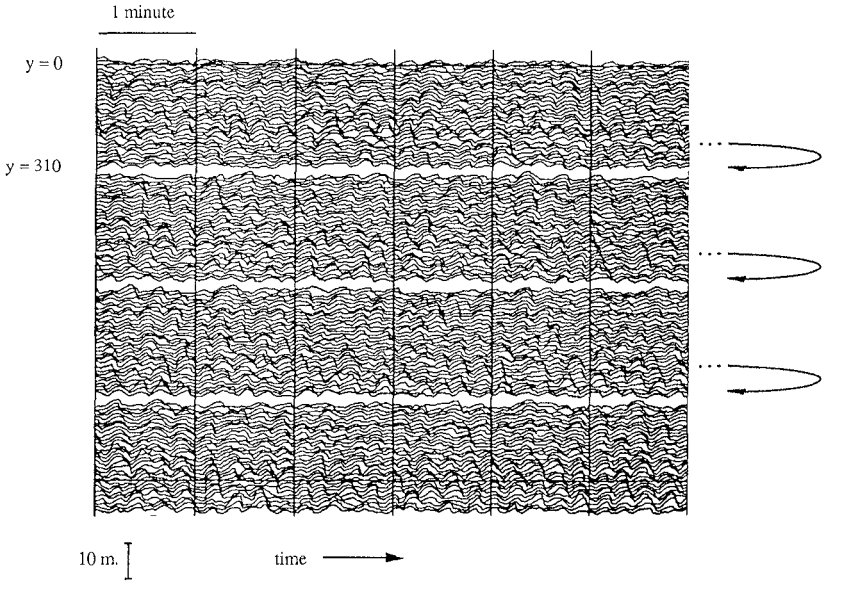

Figure 2. Example swash time series from one data run. Four non-contiguous segments are shown, each of six minute duration. For each segment, 32 adjacent transects are plotted. The longshore coherence and phase of incident wave motions is apparent. 10 m vertical swash scale is shown at bottom.

Spectra were calculated for all transects. Representative examples are shown in figure 4. In each case the peak period observed in 8 m depth is listed above the spectrum, and indicated by an arrow on the plot. For runs GD097 and GD105, there was significant energy at the incident peak. By contrast, for runs GM133 and GM143 (both near low tide) the high frequency incident waves are dissipated over the sand bar so that the spectral peak occurs at a period of about 15 seconds with some lower frequency energy present. GD097 and GD105 also show interesting (and statistically significant) peaks at lower frequency, with a representative period being 35-40 seconds. Intriguingly, this is roughly the period appropriate to an infragravity wave

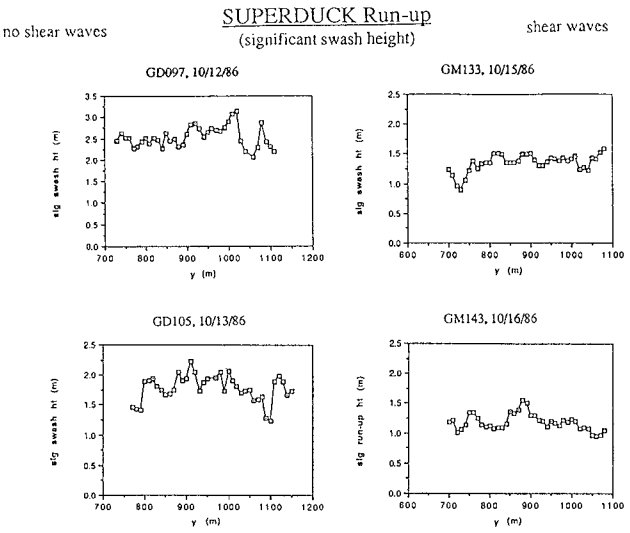

Figure 3. Longshore variability of significant swash height for each of the four selected data runs.

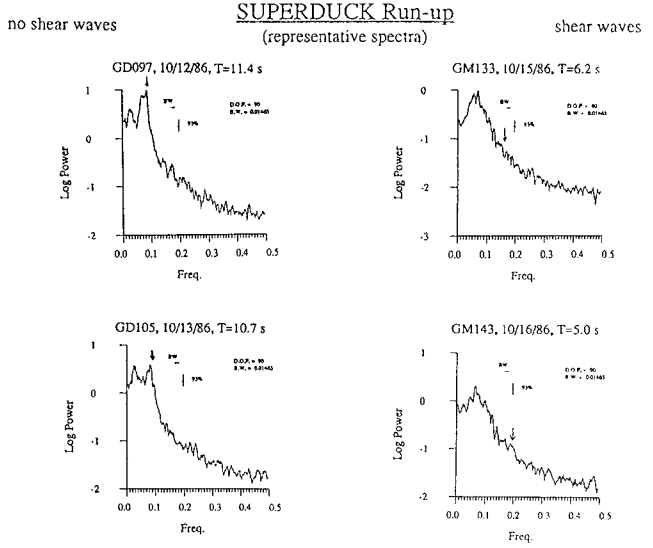

Figure 4. Spectra of swash for selected longshore transects, one for each of the four data runs. Peak periods from offshore pressure gauges are listed above each spectrum and are indicated by arrows on the plots. 90 degrees of freedom.

with a first node at the location of the observed sand bar. Examination of spectra over the length of the "array" shows a smooth variability in the lower frequency peak, suggesting some longshore standingness to this energy. This will be the subject of further work. In no case was the significant energy concentration in the very lowest frequencies associated with the FIG band.

Frequency-wavenumber results

In calculating f-k spectra from current meter measurements, a limited number of instruments (7) were deployed in a configuration optimized to the IMLE spectral analysis technique. In our case, adding "instruments" to the dataset simply involves specifying additional longshore transects to be digitized, and we have arbitrarily specified an array of 39 equally-spaced locations. However, due to technical aspect of the stability of the IMLE analysis, results are best if a subset of 7 transects are chosen, using the same lag spacing as was used for the current meter array. Of course, with so many transects, there are a number of potential choices. Figure 5 illustrates the

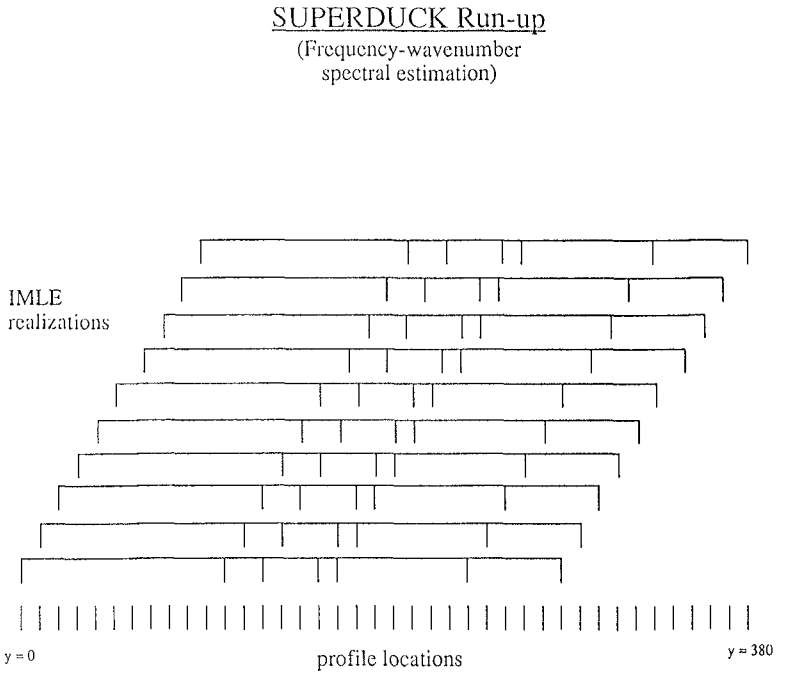

Figure 5. Schematic of "longshore array realizations" used in the analysis. The 39 available transects are shown equally-spaced at the bottom of the figure. Lines above indicate selected arrays for IMLE spectral analysis. Results from the 10 realizations are averaged to yield the final f-k spectra.

options, with the 7 sensor configuration shifted progressively in the longshore. When f-k spectra were calculated for each of these realizations, the basic structure of the spectra were similar, but there was also a great deal of noise that confused the interpretation. To combine the realizations and reduce the noise, the raw f-k spectral data were averaged for the 10 realizations shown in figure 5, yielding a much better result. (We note that many other array designs are also possible and could also be averaged into the result. The simplest of these would just be a reversal of the array. The independence of more and more permutations must gradually decrease, although, at this point, we have not pursued a rigorous quantification of the amount of averaging that is useful. Nor is it clear that averaging the wavenumber spectral results is preferred since IMLE calculations are nonlinear. Averaging of the cross-spectral matrix would be preferred and will be pursued in the future).

Figure 6b shows the resulting averaged f-k spectrum for run GM133, judged the highest quality of our data runs and also one for which shear waves were very clearly observed in the current meter records (figure 6a). Only the sub-incident frequencies are shown. The dispersion lines for modes 0, 1, 2 and cutoff mode edge waves, calculated to account for the true bathymetry as well as the presence of a mean longshore current, are shown to guide the eye.

Several features are seen. In general, there is a significant amount of energy at low wavenumbers, consistent with results from cross-shore velocity data shown in figure 6a. However, there are also clear suggestions of mode 0 edge wave energy propagating in both the southward (positive wavenumber) and northward (negative wavenumber) directions. Interestingly, the modes are asymmetric with respect to the zero wavenumber axis. This result is both predicted by the theoretical dispersion lines, and observed in the data. Identification of possible higher mode edge waves from this diagram is possible, but requires an active imagination.

Figure 7 is an alternate presentation of the same run-up spectrum. However, instead of relying on an algorithm to pick significant peaks in the spectrum, all data are shown with a shading linearly proportional to their energy density (note that each frequency band is still normalized to unit energy so that the shading density indicates relative concentration of energy within the frequency band). When viewed at a distance and with a partial squint, the concentrations of energy along curved dispersion lines are more apparent, with the two modes noted previously being relatively obvious and higher modes being somewhat distinguishable. The asymmetry due to the longshore current is quite obvious.

Figure 6a also clearly shows the region of shear wave energy from the cross-shore velocity data, as the linear feature on the positive wavenumber side of the spectrum. The concentration of energy in the shear waves is evident, particularly at the lower frequencies associated with the FIG band ($<10^{-2}$ Hz). By contrast, the same region, outlined in the run-up spectrum of figure 6b, shows no concentration of energy lying along this ridge. Some energy is observed in the lower frequency, higher wavenumber region (beyond mode 0 edge waves), but there is no correspondence between the f-k location of that energy and the location of the obvious shear waves in the current

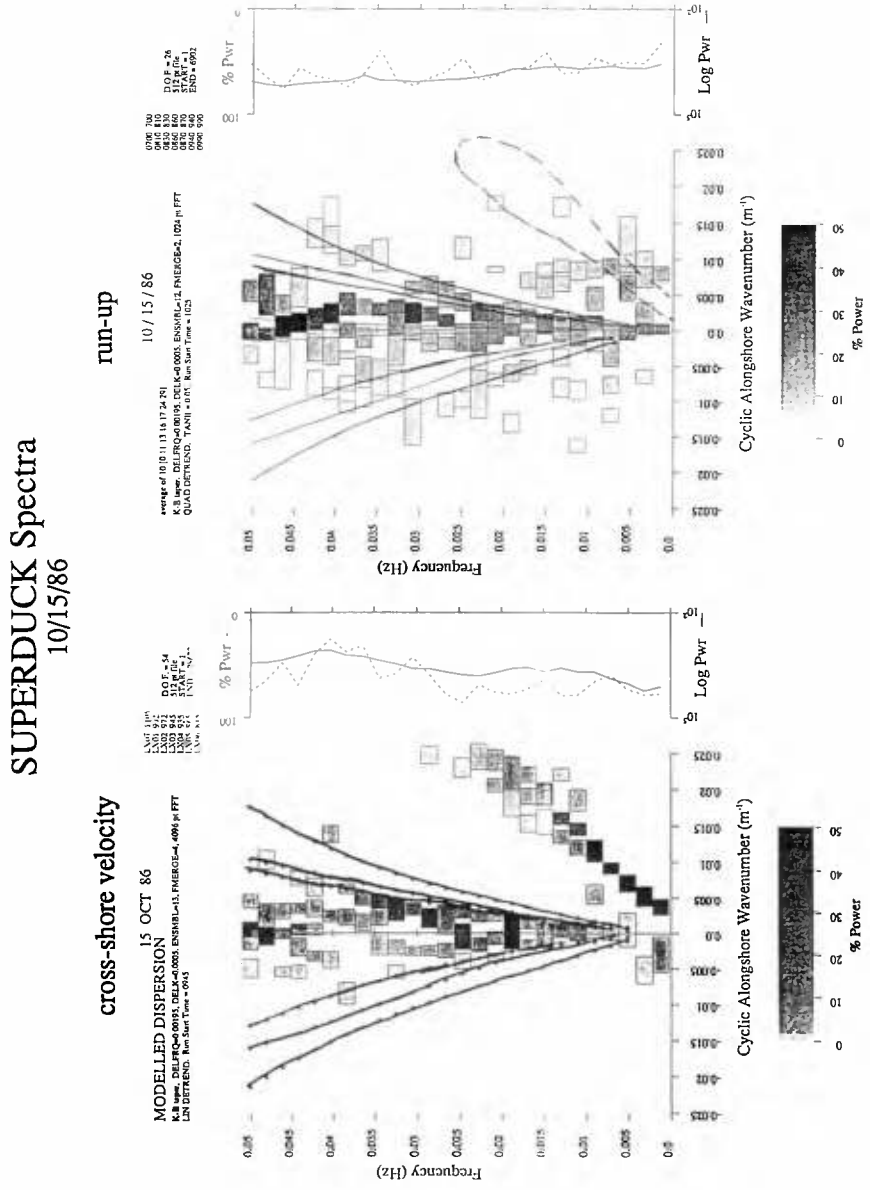

Figure 6. Frequency-wavenumber spectra for a) cross-shore velocity, and b) run-up for 10/15/86. Edge wave mode lines are for modes 0, 1, and 2 and include effects of true bathymetry and mean longshore current. Shear waves are clear in the velocity data, but are absent in run-up.

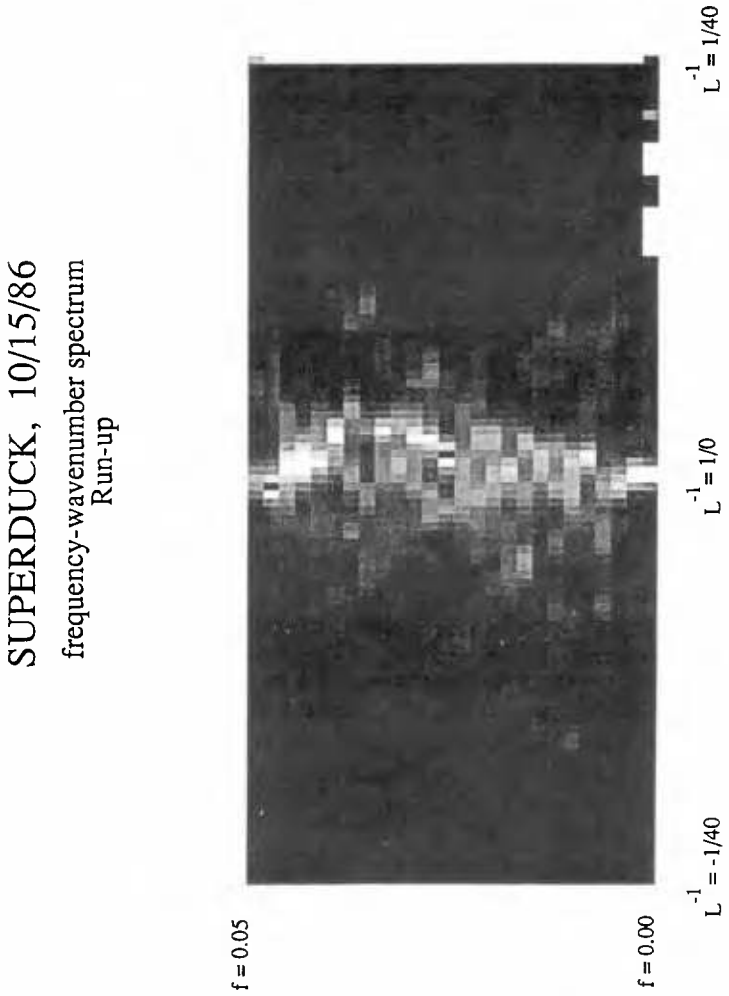

Figure 7. Frequency-wavenumber spectrum for 10/15/86. These are the same data as figure 6b) but the spectral estimates have been shaded for all f-k bins and energy concentrations are indicated by whiteness. Low mode edge waves are shown by the light color ridges curving up into plus and minus wavenumber space.

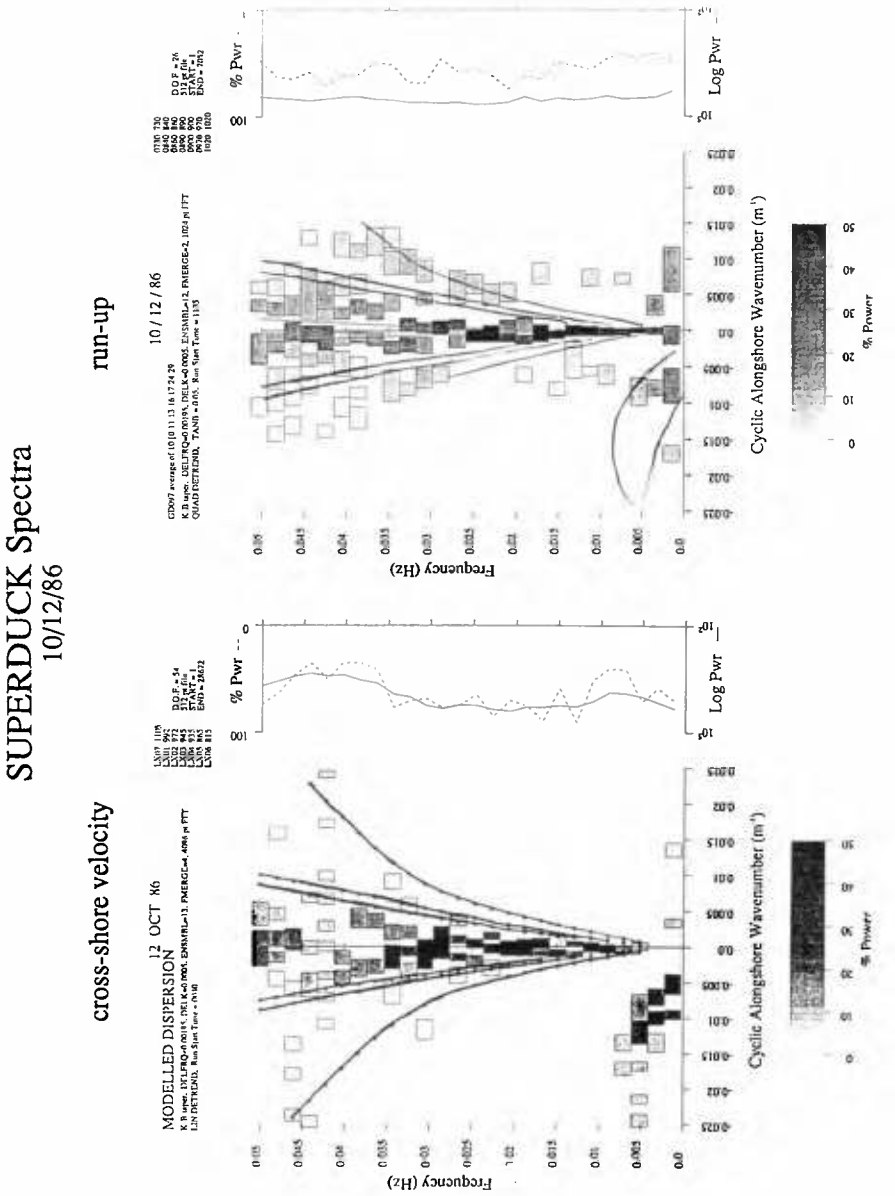

Figure 8. Frequency-wavenumber spectra for a) cross-shore velocity, and b) run-up for 10/12/86, a day for which little shear wave energy was observed in the velocity data. Edge wave mode lines are for modes 0, 1, and 2 and include effects of true bathymetry and mean longshore current. Run-up data clearly shows low mode edge wave energy, but little in the shear wave region.

meter data. At present, we do not know what the observed region of energy represents.

Figure 8 shows f-k spectra for October 12 (run GD097) for the cross-shore velocity data (figure 8a) and for run-up (figure 8b). Again, low mode edge waves are visible in the run-up data, even more than in the cross-shore velocity spectrum. While this run was specifically chosen as one for which shear wave energy was a minimum, we still see a slight concentration in the velocity data at very low frequencies and large negative wavenumber. Again, the same region, marked on the run-up spectrum, shows no particular concentration of energy.

The absence of low-frequency, high-wavenumber energy in the run-up data supports our hypothesis that shear waves are, in fact, just that; shear waves. These motions appear to obey the rigid lid assumption, showing no significant sea surface elevation signal despite large concentrations of energy in velocity time series.

Conclusions

Examination of the sea surface elevation signal (represented by swash time series) at sub-incident band frequencies has shown the presence of a variety of expected gravity wave motions including leaky modes (low wavenumber energy) and low mode edge waves. However, even under conditions when shear wave energy was extremely pronounced in velocity data taken 50 m offshore, there is no indication of such signals in the swash data. This supports the rigid lid assumption made in the theory; these low-frequency high-wavenumber motions appear to be vorticity signals with no significant sea surface elevation signal.

Acknowledgments

We would like to thank Paul O'Neill for the enormous amount of work he put into developing the image processing hardware and software, and in digitizing the data runs. Once again, we would like to acknowledge the excellent work of the Army Corps FRF staff during the SUPERDUCK experiment, and the efforts of Col. Grum in obtaining funding for the tower at Duck. Much of the theoretical and conceptual understanding of this problem has resulted from discussions with Tony Bowen. Funding for this work was from the Office of Naval Research, Coastal Sciences program under contract N00014-90-J-1118.

References

Bowen, A.J. and R.A. Holman, 1989: Shear instabilities of the mean longshore current,1. Theory. J. Geophys. Res., 94, (C12), 18023-18030.

Oltman-Shay, J.M, Howd, P.A. and W.A. Birkemeier, 1989: Shear instabilities of the mean longshore current, 2. Field observations. J. Geophys. Res., 94, (C12), 18031-18042.